The 6th International Supercritical CO2 Power Cycles Symposium
March 27 - 29, 2018, Pittsburgh, Pennsylvania

Channel Structure Influence on the Thermal-Hydraulic Performance of Zigzag PCHE

Yichao Gao
Master Student
Xi'an Jiaotong University
Shaanxi, China

Wenkai Xia
Doctor Student
Xi'an Jiaotong University
Shaanxi, China

Yaowu Huo
Doctor Student
Xi'an Jiaotong University
Shaanxi, China

Yiping Dai
Professor
Xi'an Jiaotong University
Shaanxi, China

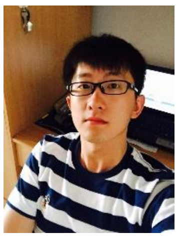

Yichao Gao

2011-2015, B.S. in Power Engineering, Xi'an Jiaotong University, Shaanxi, China
2015-Present, M.S. in Power Engineering, Xi'an Jiaotong University, Shaanxi, China

ABSTRACT

Printed Circuit Heat Exchanger (PCHE) is a very promising flat plate heat exchanger. Based on the PCHE model of Tokyo Institute of Technology, CFD method was used to measure the two fin angles which were 32.5° and 40.0° of the zigzag channels, the simulation shows a good agreement with the experiment results in local heat transfer, Nusselt number and friction factor.

The channel structure influence on the thermal-hydraulic performance of PCHE was studied, including 1.0-6.0mm channel width, 5°-60° fin angle, and six types of fin length, which were 27mm×2, 18mm×3, 9mm×6, 6mm×9, 3mm×18 and 2mm×27. The heat transfer and pressure drop increases with the decrease of channel width and the increase of fin angle. The 1.0-2.0mm channel width and 20°-45° fin angle are recommended. It indicates that the fin length is not as small as possible. 3mm fin length is the turning point and is favorable for its optimal heat transfer and relatively limited pressure drop.

Keywords: supercritical carbon dioxide; printed circuit heat exchanger; channel width; fin angle; fin length

1 Introduction

Printed Circuit Heat Exchanger (PCHE) is a compact heat exchanger with excellent heat transfer effectiveness[1], which was released in Australia in 1980. In 1985, PCHE was first used by Heatric in the refrigeration cycle in UK, representing the beginning of the commercialization of PCHE.

The fluid channels of the PCHE are formed by photochemical etching process on a metal plate. The conventional cross-sectional shape of the channel is semicircle with the diameter of 1.0-2.0mm, and different plates are stacked together by diffusion bonding to assemble the heat exchanger[2], as shown in Fig.1[3].

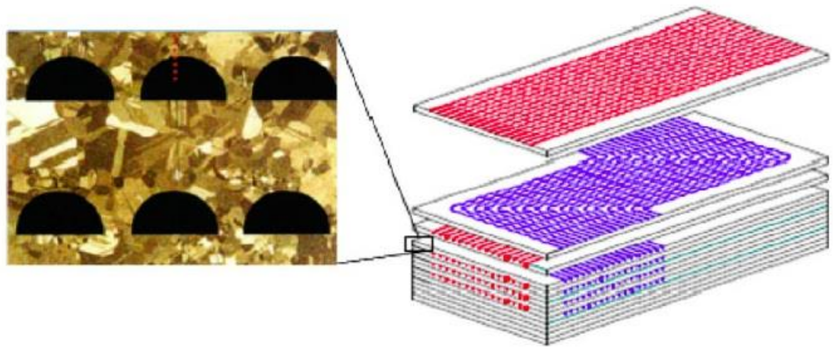

Figure.1. PCHE Channel Cross Section and Core Structure

PCHE can meet the heat transfer process of high pressure, high effectiveness, less leakage, compact structure, and so on. The maximum pressure that it can withstand is 60MPa, while the maximum temperature is 900℃, the effectiveness is over 0.9, and some are even as high as 0.98. At the same heat load and pressure drop, the volume of PCHE is 1/6-1/4 of the conventional shell and tube heat exchanger, and the average unit mass heat load reaches to 200kg/MW, and the heat transfer area density is up to 2500m^2/m^3.

Due to its compactness and good heat transfer properties, PCHE is being used in a wide range of industrial fields, such as chemical processes, fuel processing, aviation, aerospace and nuclear energy, which is a very promising candidate for the intermediate heat exchanger (IHX) in high temperature gas-cooled reactors (HTGRs) and sodium-cooled fast reactors (SFRs).

There are four types of PCHE according to the shape and layout of different flow channels: flat, zigzag, S-shaped and airfoil. Conventional PCHE flow channels are continuous semicircular zigzag corrugated channels, each of which can be used as a channel with many bends, where eddy currents, counter current, and vortices at corners improve fluid heat transfer performance and also increase the pressure drop. Therefore, some researchers have been interested in studying the internal heat transfer and flow properties in PCHE with different channel structures.

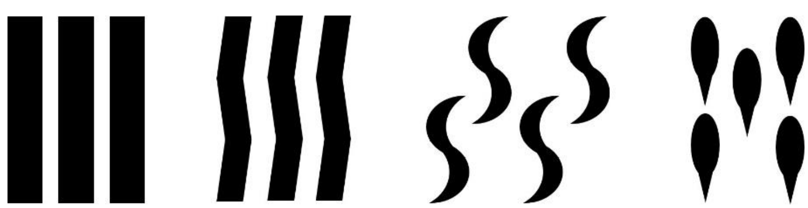

Figure.2. Different PCHE Flow Channels

Nikitin et al.[4] conducted an experiment on the flow and heat transfer performance of supercritical carbon dioxide in the conventional zigzag corrugated channel PCHE. The results show that the local heat transfer coefficient and pressure drop coefficient of the fluid is a function of the Reynolds number (*Re*).

Ngo et al.[5] designed a sinusoidal S-ribbed corrugated structure that simplified the heat transfer between the carbon dioxide and water sides to a single heat transfer unit and made numerical calculation. The results show that the volume of the PCHE can be reduced to 1/3 compared with that of the conventional zigzag corrugated channel, the pressure drop on the carbon dioxide and water side can be reduced by 37% and 90%, respectively.

Kim et al[6]. studied the heat transfer and pressure drop of supercritical carbon dioxide in a new PCHE, of which the fin structure is the NACA0020 streamlined wing. The results show that the new PCHE has the characteristics of large heat transfer area and uniform flow. The total heat transfer rate per unit volume is basically the same as the conventional zigzag PCHE, but the pressure drop is only 1/20 of the conventional PCHE.

Tsuzuki et al[7]. proposed a PCHE with S-shaped fin structure. By studying the influence of the fin length and fin angle on the pressure drop and heat transfer performance, a more optimized flow path structure was obtained. The pressure drop of the new channel structure is 20% of the conventional zigzag structure with the same heat transfer effectiveness, and the pressure drop is reduced by reducing the vortex at the elbow and reverse flows.

To sum up, it can be found that improving PCHE channel structure and reducing pressure drop on the basis of improving heat transfer are the research emphases, which is of great significance for improving the overall performance of heat exchanger. In the experiments, it is very difficult to measure the local flow parameters in the micro-scale channels. Therefore, CFD (Computational Fluid Dynamics) is widely used for doing research on PCHE.

2 Model Establishment

The experiment model of TIT (Tokyo Institute of Technology) was used in this paper, as shown in Fig.3. The PCHE volume is $71\times76\times896mm^3$, including 144 hot channels and 66 cold channels. The diameter of the hot and cold channel is 1.90mm and 1.80mm, respectively. The double banking configuration is adopted to ensure the same velocity for hot and cold channels under the condition that the volume flow rate of hot fluid is about twice of that in cold fluid.

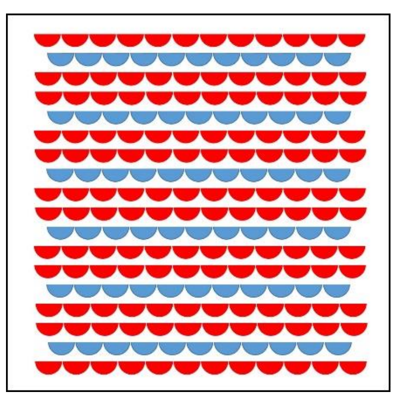

Figure.3. PCHE Cold and Hot Channels Arrangement

2.1 Model Simplification

In the experiments conducted by Nikitin and Ishizuka et al.[8], the fin angle of the hot and cold channel are 32.5° and 40.0°, making the cold channel 10% longer than the hot channel, as shown in Fig.4. In order to facilitate the boundary conditions setting of the PCHE, the length of the hot and cold channels are considered to be the same. The fin angle of 32.5° and 40.0° for both hot and cold channels were established[9], as shown in Fig.4. Because of the channel arrangement in the PCHE, it is not necessary to build the entire experiment model. Instead, one PCHE unit composed of two hot channels and one cold channel is established with periodic boundary conditions, which can simulate the entire PCHE heat transfer situation accurately, as illustrated in Fig.5.

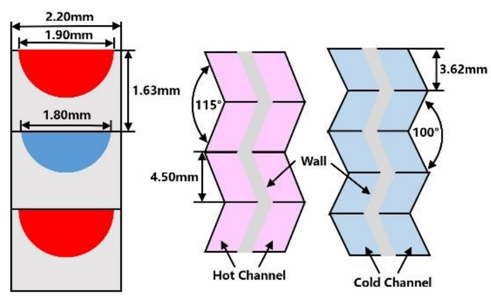

Figure.4. PCHE Channel Unit Structure Parameters

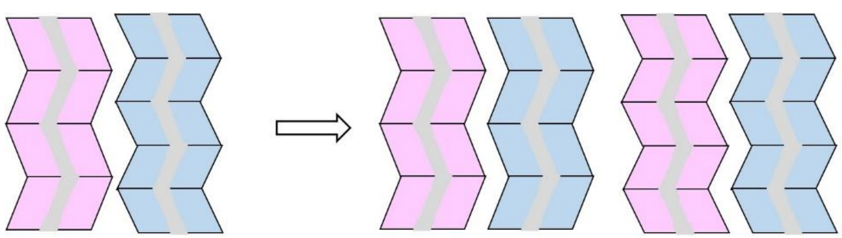

Figure.5. Experiment Model Simplification

In addition, the channel length has also been simplified from 896mm to 54mm. With this simplification, the inlet temperature of the cold fluid needs to be adjusted from 108°C to 221.8°C, which proves to be a good match with the experiment in the numerical study of Kim et al.[10], as shown in Fig.6. The actual range of PCHE unit studied in this paper is the part corresponding to the X-axis 0-0.054m.

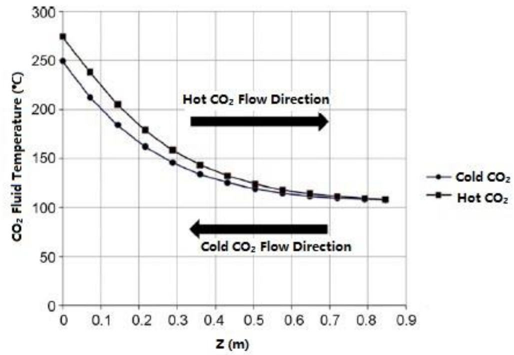

Figure.6. Kim Simulation of Cold and Hot Fluid Temperature Change along the Wall

2.2 Meshing

Solidworks software was used to generate the PCHE model. Surfaces From Edges and Fill module in the Ansys design modeler was used to generate the SCO_2 Fluid. Tetrahedral network was used to mesh the PCHE and the SCO_2 fluid. For the boundary layer between the solid and fluid, Inflation module was applied and the first layer thickness of SCO_2 fluid is 0.01mm. Five rows were created with a growth rate of 1.2, the total thickness of the boundary layer is 0.0744mm, according to the experience of Kim et al[11]. Grid independent test was carried out and results are listed in Table 1. When the number of elements reaches to 1069880, heat transfer coefficient on both sides converged. Hence, the 1069880 elements was chosen as a reference grid considering the simulation time and accuracy.

Table 1. PCHE Grid Independence Test

Description	Mesh Elements	HTC in Cold Side	Relative Deviation	HTC in Hot Side	Relative Deviation
Coarse	378410	6701.03	-12.1%	3306.05	-11.3%
Medium	586652	7154.37	-6.1%	3459.75	-7.1%
Medium-Fine	824445	7347.5	-3.6%	3431.81	-7.9%
Fine	1069880	7542.77	-1.1%	3647.83	-2.1%
Good	1235863	7622.85	0.0%	3726.09	0.0%

Note: Where HTC is the heat transfer coefficient

2.3 Boundary Conditions

Post-processing was performed on Ansys CFX. The structural material of PCHE is steel, which has the thermal conductivity of 16.2W/(m·K), and the heat transfer mode is thermal energy. CO2RK was chosen for SCO_2 with the pressure ranging from 1MPa to 20MPa, temperature ranging from 100K to 1000K. The total energy equation was used for heat transfer and the k-ε turbulence model is adopted which has good convergence and is widely used in engineering. Inlet temperature and pressure for hot and cold side are 280℃, 3.2MPa and 221.8℃, 10.5MPa, respectively. 5% turbulence intensity was applied. Mass flow rate control was used for outlet conditions, which is from 30kg/h to 390kg/h, with an increment of 15kg/h. The top and bottom, left and right surfaces of PCHE are set as translational periodicity boundary condition and the front and rear surfaces are set as adiabatic boundary conditions. For the boundary layer between

PCHE and SCO_2 fluid, general connection was used, as illustrated in Fig.7. The first-order high-precision convergence mode was adopted and the convergence precision is 10^{-4}.

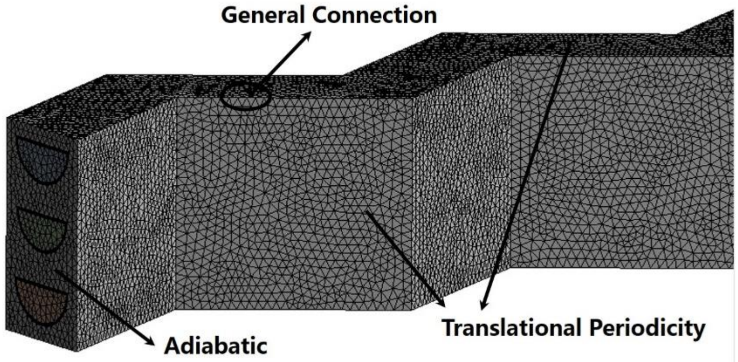

Figure.7. PCHE Meshing and Boundary Settings

3 Comparison of Simulation and Experiment

Two key metrics for measuring PCHE performance are heat transfer and pressure drop. Local heat transfer coefficient *h* and Nusselt number were used to measure the heat transfer performance. Nusselt number characterizes the ratio of the fluid thermal conductivity to the convective thermal resistance. The larger Nusselt number indicates better heat transfer performance of the PCHE:

$$Nu = \frac{h_{av} D_h}{\lambda_{av}}$$

h_{av} and λ_{av} represent the average convective heat transfer coefficient and average thermal conductivity of the fluid, respectively.

Pressure drop was defined by the subtraction of inlet and outlet pressure:

$$\Delta P = P_{in} - P_{out}$$

In addition, the friction factor *f* can also be used to measure the pressure drop. The larger *f* indicates greater flow resistance：

$$f = \frac{P_{in} - P_{out}}{2\rho_{out} V_{out}^2} (\frac{D_h}{L})$$

P_{in} and P_{out} are the PCHE channel inlet and outlet pressure, respectively. ρ_{out} and V_{out} are the SCO_2 outlet density and velocity.

CFD simulation results are compared with the experiment results in this chapter. Some researchers give the empirical formula for the local heat transfer coefficient *h*, Nusselt Number and friction factor *f* related to the Reynolds number, Prandtl number and channel structure, which are shown in the following table.

Table 2. Empirical Formula of Local Heat Transfer Coefficient, Nusselt Number and Friction Factor

Researchers	Local HTC or *Nu*	Friction Factor	Application Scope
Nikitin	$h_{hot} = 2.52\,\mathrm{Re}^{0.681}$ $h_{cold} = 5.49\,\mathrm{Re}^{0.625}$	$f_{hot} = -1.402\times 10^{-6}\,\mathrm{Re} + 0.04495$ $f_{cold} = -1.545\times 10^{-6}\,\mathrm{Re} + 0.09318$	$2800 \le \mathrm{Re} \le 5800$ $6200 \le \mathrm{Re} \le 12100$
Ishizuka	$h = 0.2104\,\mathrm{Re} + 44.16$	$f_{hot} = -2.0\times 10^{-6}\,\mathrm{Re} + 0.0467$ $f_{cold} = -2.0\times 10^{-6}\,\mathrm{Re} + 0.1023$	$2400 \le \mathrm{Re} \le 6000$ $5000 \le \mathrm{Re} \le 13000$
Ngo	$\mathrm{Nu} = 0.1696\,\mathrm{Re}^{0.629} \times \mathrm{Pr}^{0.317}$	$f_{hot} = 0.3390\,\mathrm{Re}^{-0.158}$ $f_{cold} = 0.3749\,\mathrm{Re}^{-0.154}$	$3500 \le \mathrm{Re} \le 22000$ $0.75 \le \mathrm{Pr} \le 2.2$
Hesselgreaves	$\mathrm{Nu} = 0.4\,\mathrm{Re}^{0.64}\,\mathrm{Pr}^{1/3}\left(\frac{2b}{a}\right)^{0.75}$	$f = 4.8\,\mathrm{Re}^{-0.36}\left(\frac{2b}{a}\right)^{1.5}$	$10^4 < \mathrm{Re} < 10^5$

Note: Where *a* is the fin length and *b* is the channel width.

3.1 Heat Transfer Comparison in Cold and Hot Side

Due to the same thermal-hydraulic performance between the 32.5° and 40.0° fin angle of the PCHE, 32.5° fin angle was used for description.

As illustrated in Fig.8, (a), (b), (c) and (d) represent the CFD results of the local heat transfer coefficient and Nusselt number compared with the experiment of different researchers, respectively. The ranges of the existing correlations were extended up to Reynolds number 60000. Because of the similar flow velocities of hot and cold fluids, while the cold fluid density is much higher than that of hot fluids, the range of Reynolds numbers of cold fluids is broader than that of hot fluids.

For the local heat transfer coefficient *h*, the CFD result is in good agreement with the experiment results of Nikitin and Ishizuka at low Reynolds numbers. With the increase of Reynolds number, the CFD result is basically consistent with the trend of Ishizuka experimental result, while the deviation with Nikitin experimental result increases gradually. Taking CFD results as a reference, Nikitin's experimental results can be applied to low Reynolds numbers, while Ishizuka's experimental results is recommended at both low and high Reynolds numbers.

For the Nusselt number, the CFD result agrees with that of Ngo at low Reynolds number, while at high Reynolds number, the difference between Ngo and CFD result become obvious. Hesselgreaves[12] experimental results is applicable at high Reynolds numbers. With the increment of Reynolds number, CFD results and Hesselgreaves experiment results become more consistent.

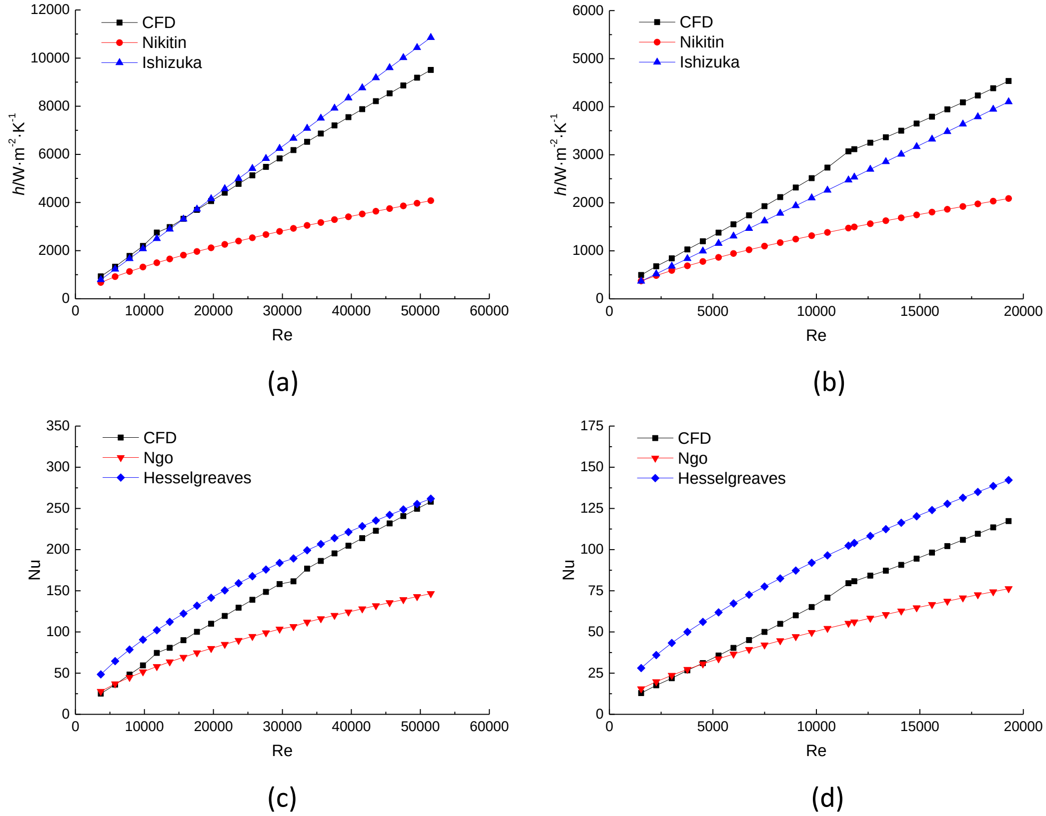

Figure.8. Heat Transfer Performance at Fin Angle 32.5° in Cold and Hot Side

3.2 Pressure Drop Comparison in Cold and Hot Side

As shown in Fig.9, it indicates that the CFD results are in good agreement at fin angle 32.5° with the experiment results from four researchers. The friction factor decreases gradually and approaches a stable value with the increase of the Reynolds number. For the experimental results of Hesselgreaves, the friction factor is larger compared with the CFD results. For Nikitin and Ishizuka, the experimental results are more credible when the Reynolds number is low, while at high Reynolds number, the friction factor calculated by the empirical formula is 0 or negative, which is possibly inaccurate.

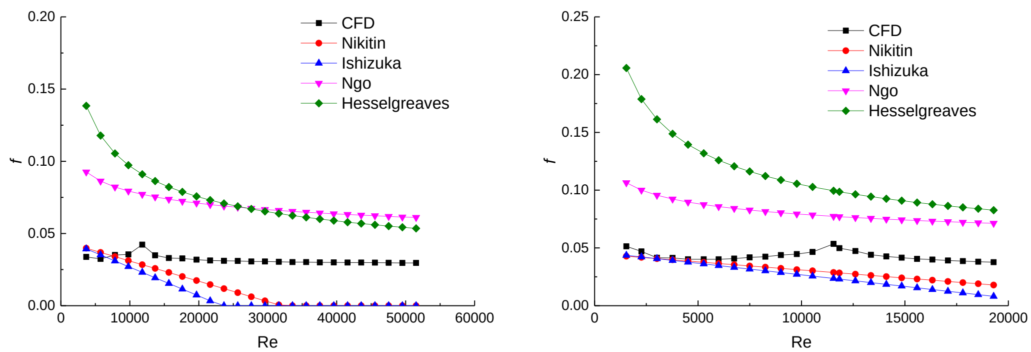

Figure.9. Pressure Drop at Fin Angle 32.5° in Cold and Hot Side

3.3 Relative Deviation of Heat Transfer and Pressure Drop

The relative deviation of heat transfer and friction factor are shown in Table 3 and Table 4. By comparing the CFD results with the experimental data, it is concluded that the relative deviation are acceptable. The accuracy of the CFD method in studying the thermal-hydraulic performance of the PCHE is proved.

Table 3. Relative Deviation for Heat Transfer and Pressure Drop at Fin Angle 32.5°

32.5°	Ishizuka hot	Ishizuka cold	Ngo hot	Ngo cold	Hesselgreaves hot	Hesselgreaves cold
h or *Nu*	+21.1%	+12.9%	+33.0%	+20.6%	-21.1%	-13.8%
f	+8.3%	-10.9%	-45.7%	-55.8%	-53.1%	-52.3%

Table 4. Relative Deviation for Heat Transfer and Pressure Drop at Fin Angle 40.0°

40.0°	Ishizuka hot	Ishizuka cold	Ngo hot	Ngo cold	Hesselgreaves hot	Hesselgreaves cold
h or *Nu*	+38.5%	+37.7%	+56.6%	+58.6%	-19.7%	-2.4%
f	+5.8%	-10.9%	-10.4%	-10.7%	-35.2%	-8.3%

4 PCHE Channel Structure Influence on Heat Transfer and Pressure Drop

In general, an effective way to improve the performance of the heat exchanger is to increase the average heat transfer temperature difference and the flow rate. However, some parameters such as temperature, pressure and flow rate of hot and cold fluid are often given and cannot be changed in the engineering, therefore, changing the heat exchanger structure is the most reasonable way to increase the heat transfer. For the zigzag PCHE, the channel width, fin angle, and fin length determine its basic structure, all of which have a certain effect on heat transfer and pressure drop.

4.1 Channel Width Influence on PCHE Heat Transfer and Pressure Drop

In order to explore the channel width influence on heat transfer and pressure drop of PCHE, this chapter is based on the 32.5° fin angle and 4.5mm fin length. Considering the conventional PCHE channel width is generally 1.0-6.0mm, 1.0mm to 6.0mm channel width was created with an increment of 1.0mm.

The mass flow rate was set from 300kg/h to 600kg/h with an increment of 30kg/h. The pressure drop is greater under large flow conditions and it is easier to judge whether the pressure drop is beyond the design range. In general, the pressure drop is within 1.5% of the inlet pressure that meets the design requirements.

As shown in Fig.10, the convective heat transfer coefficient increases with the increase of mass flow rate under the same channel width condition, showing a linear growth relationship. At the same mass flow rate, the convection heat transfer coefficient decreases significantly with the increase of channel width. In the range of 300kg/h to 600kg/h, 1mm channel width PCHE has a convective heat transfer coefficient of 19000-32000 W/(m^2·K), which is an excellent heat transfer performance. The heat transfer efficiency drops sharply when the channel width is increased from 1mm to 2mm. For the 6mm channel width, the heat transfer coefficient varies from 900-1700 W/(m^2·K), far less than the heat transfer performance of 1mm channel width, which is only about 5% of the former.

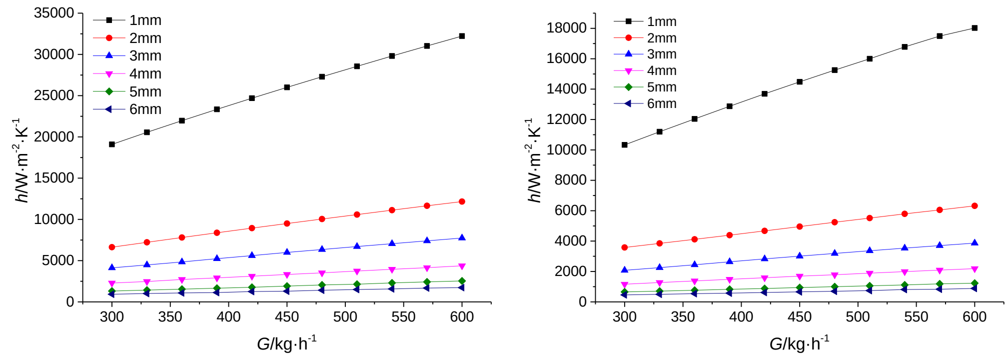

Figure.10. Channel Width Influence on PCHE Heat Transfer

Three representative channel width are chosen for analysis due to the similar heat transfer and flow characteristics, as illustrated in Fig.11. It indicates that the convection heat transfer coefficient is obviously larger near the channel corner. The fluid flow direction changes and the disturbance increases significantly at the corner. The heat transfer was enhanced with the boundary layer destroyed. In addition, the flow velocity with small channel width is larger at the same mass flow rate, and the turbulent state is more likely to develop from laminar to turbulent flow, which also improves the convection heat transfer.

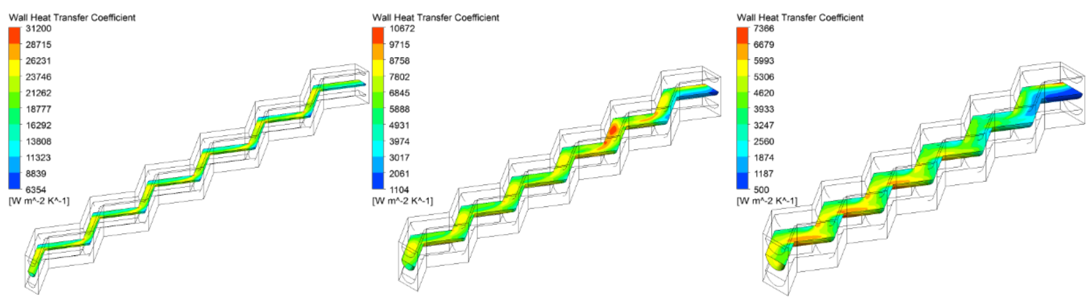

(a) 1mm, 300kg/h, cold side (b) 2mm, 300kg/h, cold side (c) 3mm, 300kg/h, cold side

Figure.11. Convection Heat Transfer Coefficient Distribution of the Typical Channel Width

As illustrated in Figure.12, the PCHE pressure drop changes linearly with the increasing of mass flow rate. When the mass flow rate increases to a certain value, the pressure drop begins to change exponentially with the mass flow rate increasing. Obviously, under the same flow conditions, pressure drop of 1mm channel width is much higher than other channel width.

Although PCHE with 1mm channel width achieves excellent heat transfer, while there is a substantial increase in pressure drop. The pressure drop of 1mm channel width has reached about 0.4MPa at 300kg/h mass flow rate, accounting for 3.5% of the inlet pressure. At the flow rate of 600kg/h, the pressure drop reaches about 1.6MPa, which is 14.5% of the inlet pressure and beyond the design requirements. It is achieved with a channel length of 54 mm, while the actual channel length is 896 mm. Excessive pressure drop can lead to excessive consumption of the pump power, affecting the thermal cycle economy.

For the PCHE of 2mm channel width, the pressure drop is 20-80kPa in the range of 300kg/h to 600kg/h, accounting for 0.6% -2.5% of the inlet pressure on the hot side, which shows that 2mm channel width is within the pressure drop design requirements. 2mm channel width PCHE can combine both heat transfer and pressure drop, which is why a large variety of PCHE channel width are designed around 2mm.

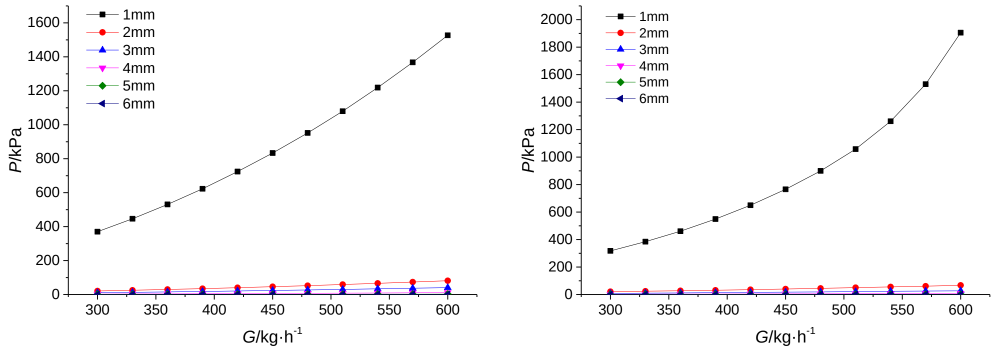

Figure.12. Channel Width Influence on PCHE Pressure Drop

For 3mm-6mm channel width PCHE, the pressure drop is small, but the heat transfer performance is poor. It indicates from Fig.13 that the cold fluid with the 2mm channel width starts to have some reversed flows at the corner, and at the 3mm channel width, the cold fluid shows clear swirl flows, reversed flows and eddies at the corner, which causes a certain extent of pressure drop, thus deteriorating the heat transfer performance.

However, it can be found that the cold fluid velocity with 1mm channel width is significantly higher than that of 2mm and 3mm. In combination with Figure.12, the pressure drop caused by wall resistance at high velocity is significantly more than that caused by the reversed flows at low velocity. The high mass flow rate is the reason that causes the pressure drop of 1mm channel width larger than other channel width, but also makes the heat transfer performance of 1mm channel width better.

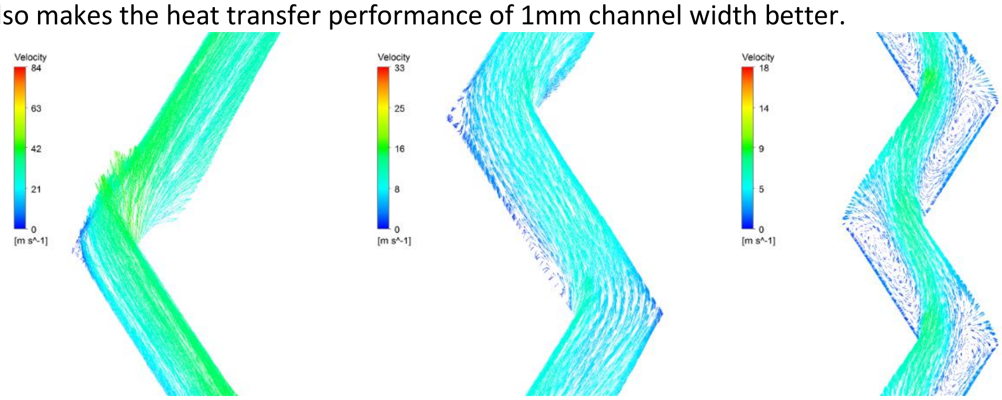

(a) 1mm, 300kg/h, cold side (b) 2mm, 300kg/h, cold side (c) 3mm, 300kg/h, cold side

Figure.13. Velocity Vector Distribution of the Typical Channel Width

After the above analysis, for some conditions that may enhance the pressure drop, such as large flow conditions and long channel length, large channel width should be used. When the mass flow rate is relatively small, or the channel length is relatively short, the pressure drop is more easily to meet the design requirements, small channel width should be considered in order to improve the heat transfer performance

4.2 Fin Angle Influence on PCHE Heat Transfer and Pressure Drop

In order to explore the influence of fin angle on heat transfer and pressure drop of PCHE, six flow conditions vary from 50kg/h-300kg/h were set based on PCHE of 2mm channel width, 4.5mm fin length. The fin angle increases from 5° to 60° with an increment of 5°.

As illustrated in Fig.14, under the same mass flow rate, the large fin angle causes more disturbance when the fluid flows through the channel corner, which improves the heat transfer performance. Therefore, the heat transfer performance increases with the fin angle gradually. It indicates that the curves of fin angle and convection heat transfer coefficient are approximately linear in the range of 5°-20°, 20°-45° and 45°-60°.

In the range of 5-20° and 45°-60°, the heat transfer performance is relatively flat with the fin angle increasing. However, in the range of 20°-45°, the slope of the curve corresponding to the fin angle and heat transfer coefficient is relatively steep, and the heat transfer increment is more obvious with the fin angle increasing. It can be found that the convective heat transfer coefficient at 60° is close to twice of that at 5°. Large fin angle has more disturbance on the fluid due to the large change of the flow direction, so the convection heat transfer coefficient is higher, as shown in Fig.15.

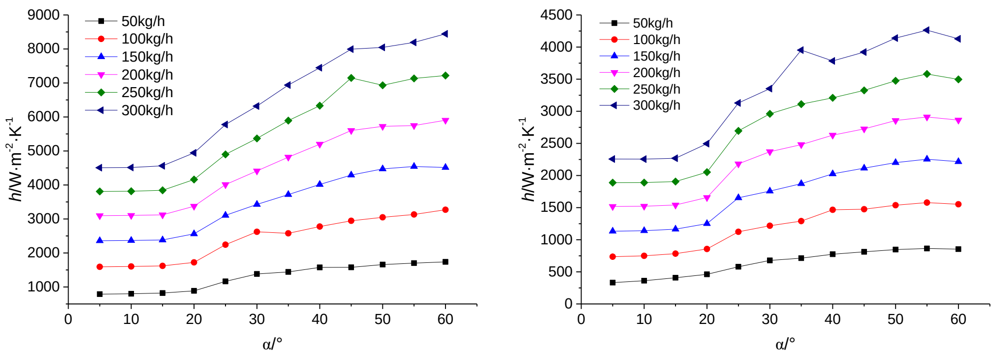

Figure.14. Fin Angle Influence on PCHE Heat Transfer

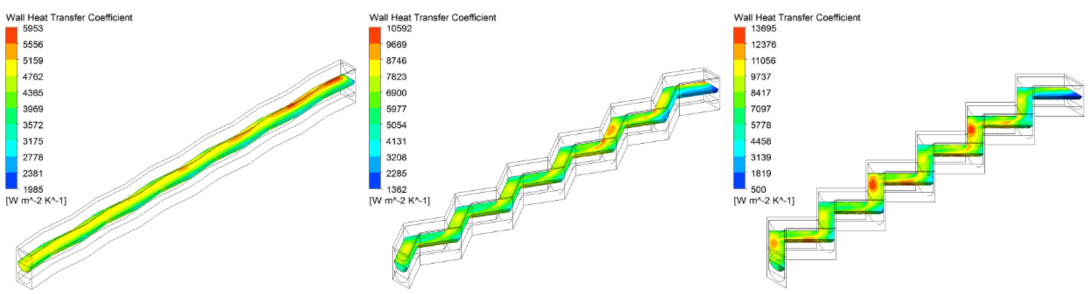

(a) 5°, 300kg/h, cold side (b) 30°, 300kg/h, cold side (c) 45°, 300kg/h, cold side

Figure.15. Convection Heat Transfer Coefficient Distribution of the Typical Fin Angle

The existence of the fin angle enhances the fluid disturbance significantly and improves the heat transfer, but also causes great energy loss inevitably when the fluid flows through the corner, that is, the pressure drop is increased. As shown in Fig.16, under the same mass flow rate, the pressure drop also increases with the increase of fin angle, while they show an exponential trend, that is different from the tendency of heat transfer coefficient and fin angle. For a mass flow rate of 300kg/h and 60° fin angle, the corresponding pressure drop is 80.1kPa, accounting for 0.76% of the inlet pressure, which is within the pressure drop design requirements. However, as the mass flow rate continues to increase or the channel length increases, it is possible to exceed the design requirement.

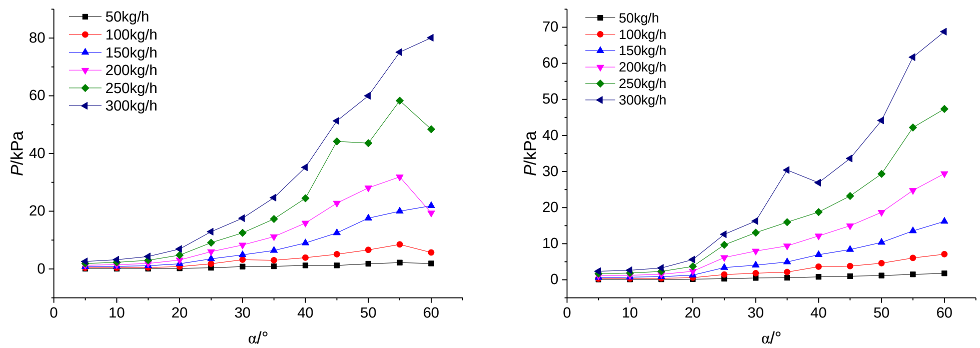

Figure.16. Fin Angle Influence on PCHE Pressure Drop

As shown in Fig.17, it can be found that the fluid velocity of 5° fin angle is the smallest, the 30° fin angle is the second, and the 45° fin angle is the maximum. Compared with the fin angles of 5° and 30°, the fin angle of 45° has greater reversed flow loss at the corners, resulted in a larger pressure drop. Combined with the Fig.14, the heat transfer performance changes little from 45° because of the reversed flow zone, while it is separated from the main flow zone and formed a relatively "vacuum" state, thus leads to the poor heat transfer performance.

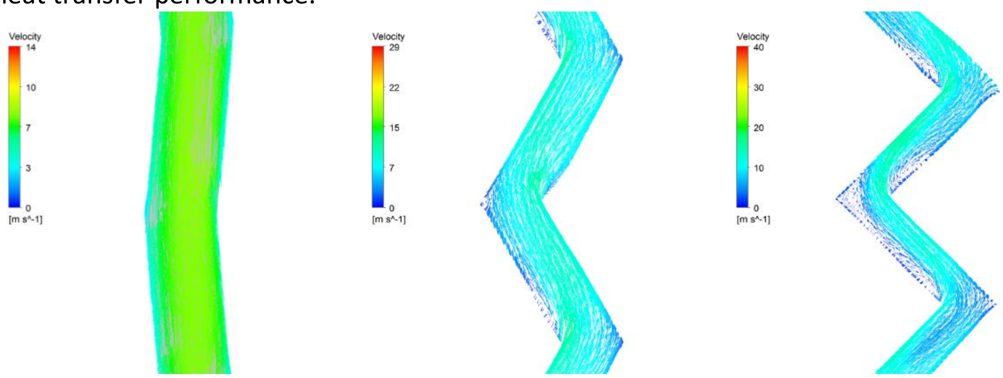

(a) 5°, 300kg/h, cold side (b) 30°, 300kg/h, cold side (c) 45°, 300kg/h, cold side

Figure.17. Velocity Vector Distribution of the Typical Fin Angle

From the above analysis, if the pressure drop meets the requirements, large fin angle has better heat transfer performance. In the range of 20°-45° fin angle, the heat transfer performance increases more obvious, while the pressure drop is relatively small, which can be focused on when designing PCHE.

4.3 Fin Length Influence on PCHE Heat Transfer and Pressure Drop

In order to explore the fin length influence on heat transfer and pressure drop of PCHE, six flow conditions vary from 50kg/h to 300kg/h were set based on 2mm channel width and 30° fin angle of PCHE. The 54mm channel length were separated into six categories, which are 27mm×2, 18mm×3, 9mm×6, 6mm×9, 3mm×18 and 2mm×27, which is illustrated in Fig.18.

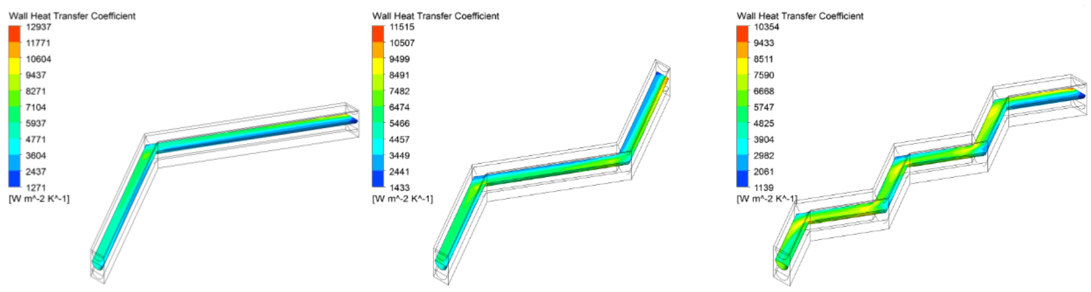

(a) 27mm×2, 300kg/h, cold side (b) 18mm×3, 300kg/h, cold side (c) 9mm×6, 300kg/h, cold side

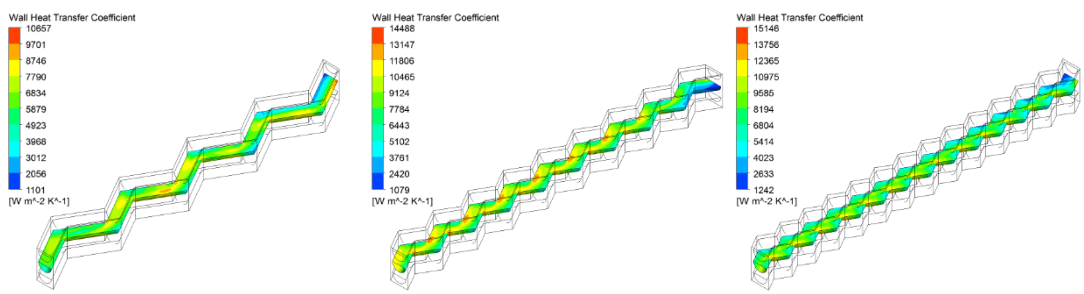

(d) 6mm×9, 300kg/h, cold side (e) 3mm×18, 300kg/h, cold side (f) 2mm×27, 300kg/h, cold side

Figure.18. Convection Heat Transfer Coefficient Distribution of the Typical Fin Length

As illustrated in Fig.19, with the decrease of the fin length, the convective heat transfer coefficient increases and reaches a peak value when the fin length is 3mm. Thereafter, the convection heat transfer coefficient shows a decreasing trend as the fin length continues to decrease. When the fin length is relatively small, there are more disturbance when the fluid flows through the corners, and the heat exchange is more sufficient. When the fin length continues to reduce, the corners becomes excessive and not sharp enough, the channels are more like the straight channels, which cannot match the heat transfer performance with zigzag channels.

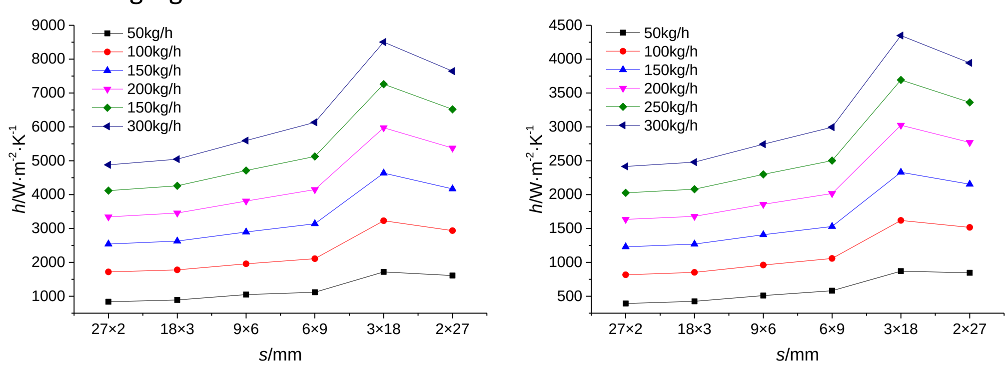

Figure.19. Fin Length Influence on PCHE Heat Transfer

As shown in Figure.20, at 3mm fin length, the pressure drop reaches to the maximum, then is begins to decrease as the fin length decreased. The mechanism is similar with that of heat transfer. When the fin length is small and the number of corners become infinite, while the flow velocity and direction change little when flow through the relatively "straight" channels, so the pressure drop is reduced and the heat transfer performance is also deteriorated.

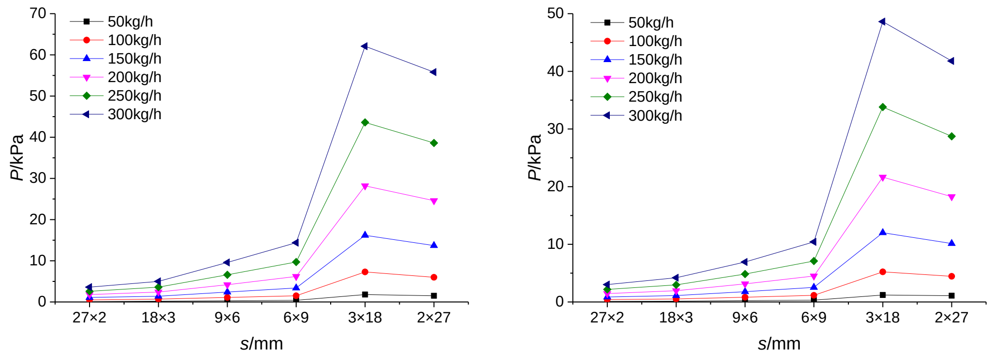

Figure.20. Fin Length Influence on PCHE Pressure Drop

It can be found from Fig.21 that the change of fin length has little effect on the speed of flow. The maximum velocity of these three types of fin length is about 30m/s and about 15-20m/s on average. However, the 3mm×18 reversed flow area is larger than 2mm×27, and the corresponding pressure drop is also larger. At the same time, it can be found that the mainstream area of 3mm×18 is longer than 2mm×27. While the mainstream area of 2mm×27 is similar to the straight flow, thus the heat transfer performance is not as good as 3mm×18. The ideal fin length should change the fluid flow direction as much as possible.

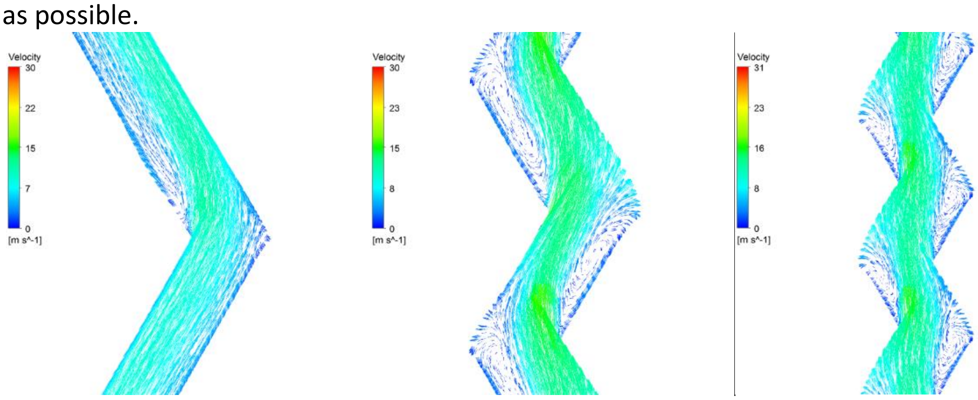

(a) 18mm×3, 300kg/h, cold side (b) 3mm×18, 300kg/h, cold side (c) 2mm×27, 300kg/h, cold side

Figure.21. Velocity Vector Distribution of the Typical Fin Length

Based on the above analysis, it indicates that the small fin length has better heat transfer performance, meanwhile the increase of pressure drop is not large. But the fin length is not as small as possible, there is also a peak performance, around 3mm fin length has the best overall performance.

5 Conclusion

This paper is based on the PCHE model of TIT. CFD method was used and compared with the experiments, which proves it accuracy and rationality. To maximize the heat transfer performance and minimize the pressure drop, channel structure influence on PCHE was studied, which are summarized as follows:

- The increase of channel width decreases the heat transfer and the pressure drop simultaneously. Under the pressure drop design requirements, small channel width has the best heat transfer effectiveness and 1.0-2.0mm channel width is recommended.

- The increase of fin angle increases the heat transfer and the pressure drop simultaneously. The heat transfer increases little in 5°-20° and 45°-60° fin angle, and the pressure drop grows fast in 45°-60°

fin angle. The 20°-45° fin angle is favorable for it combines the good heat transfer effectiveness and small pressure drop.

- The heat transfer and pressure drop increases with the decrease of fin length to a certain value, and then the trend becomes opposite. 3mm is the turning point fin length and is recommended for its optimal heat transfer performance and limited pressure drop.

6 References

1. Baek S, Kim JH, Jeong S, et al. Development of highly effective cryogenic printed circuit heat exchanger (PCHE) with low axial conduction[J]. Cryogenics, 2012, 52(7): 366-374.
2. Gezelius K. Design of compact intermedia heat exchangers for gas cooled fast reactors [D]. Massachusettes: Massachusettes institute of technology, 2004.
3. Southall, D., Le Pierres, R., Dewson, S. J., “Design Considerations for Compact Heat Exchangers”, Proceedings of ICAPP ’08, Anaheim, CA., June 8-12, 2008, Paper 8009
4. Nikitin, K, Kato Y, Ngo TL. Printed circuit heat exchanger thermal–hydraulic performance in supercritical CO2 experimental loop [J]. Int. J. Refrig, 2006, 29: 807–814.
5. Ngo T L, Kato Y, Nikitin K, et al. Heat transfer and pressure drop correlations of microchannel heat exchangers with S-shaped and zigzag fins for carbon dioxide cycles [J]. Experimental Thermal & Fluid Science, 2007, 32(2): 560-570.
6. Kim DE, Kim MH, Cha JE, et al. Numerical investigation on thermal-hydraulic performance of new printed circuit heat exchanger model [J]. Nuclear Engineering and Design, 2008, 238(12): 3269-3276.
7. Tsuzuki N, Kato Y, Ishiduka T. High performance printed circuit heat exchanger [J]. Applied Thermal Engineering, 2007, 27(10): 1702-1707.
8. Ishizuka T, Kato Y, Muto Y. Thermal-hydraulic characteristics of a printed circuit heat exchanger in a supercritical CO2 loop [C]. Avignon, France: The 11th International Topical Meeting on Nuclear Reactor Thermal–Hydraulics, 2005, October 2–6.
9. Kim S G, Lee Y, Ahn Y, et al. CFD aided approach to design printed circuit heat exchangers for supercritical CO2, Brayton cycle Application [J]. Annals of Nuclear Energy, 2016, 92: 175-185.
10. DE Kim, MH Kim. Numerical investigation on thermal–hydraulic performance of new printed circuit heat exchanger model [J]. Nuclear Engineering and Design, 2008, 238: 3269–3276.
11. Kim I H, Sun X. CFD study and PCHE design for secondary heat exchangers with FLiNaK-Helium for SmAHTR [J]. Nuclear Engineering & Design, 2014, 270(5): 325-333.
12. John E. Hesselgreaves. Compact Heat Exchangers – Selection, Design and Operation [M]. Pergamon: 2001.